Discharge and Dispersion in Water-Mist Sprays: Experimental and Numerical Analysis

Paolo E. Santangelo[a], Paolo Tartarini[a,*], Beatrice Pulvirenti[b] and Paolo Valdiserri[b]
[a] Dipartimento di Ingegneria Meccanica e Civile (DIMeC),
Università degli Studi di Modena e Reggio Emilia, Via Vignolese 905/b, 41100 Modena, Italy
[b] Dipartimento di Ingegneria Energetica, Nucleare e del Controllo Ambientale (DIENCA),
Alma Mater Studiorum – Università di Bologna, Viale Risorgimento 2, 40100 Bologna, Italy

Abstract

The present study is aimed at modeling a high-pressure water-mist spray employing two classic numerical codes. To this end, an experimental campaign has been performed both to obtain the input data for the numerical approach and to serve as a validating tool to quantify the predictive capability of the proposed models. In particular, experiments have been conducted to determine volume-flux distribution, drop-size distribution, initial velocity and spray-cone angle. Advanced laser-based diagnostics (*Malvern Spraytec* and Particle Image Velocimetry) has been employed together with simple *ad hoc* built instruments to measure these parameters over a prescribed range of high operative pressures (50-90 bar). Specific measurement methodologies have been developed to gain a proper experimental evaluation of any subject of investigation. Then, a computational simulation of the water-mist spray has been implemented in Fluent and FDS (Fire Dynamics Simulator) codes. Characteristic drop size, velocity and cone angle have been introduced as input parameters, while volume-flux distribution has been employed to compare numerical results to experimental data as a final validating task. A good qualitative agreement has been gained: the spray physics appears to be properly expressed by the proposed models. However, intrinsic limitations characterize both the experimental tools and the computational codes and may explain some still-to-be-solved discrepancies from a quantitative point of view.

Introduction

Water-mist systems are now an established promising technology in fire-protection engineering. These water-based systems are largely employed in commercial, industrial and military applications. Advancements in water-mist technology have mainly resulted from interest in Halon alternatives. Among all the research available in the open literature, it is worthwhile to mention the studies conducted by the US Navy [1-3] and by Chelliah and his co-workers [4,5] on fire-suppression efficiency of water-mist systems. However, most researches are focused on suppression mechanisms and flame-flow interactions, while only few works [6,7] have been conducted to characterize the spray features of these systems. Drop transport and associated fire-suppression performance depend on atomization and dispersion characteristics of the spray. The current study is aimed at both characterizing discharge and dispersion phenomena of water-mist sprays and providing a numerical simulation of their behavior. A typical nozzle (645 J12C B1 by *PNR Italia S.r.l.*) has been investigated in the present study: it operates at high supply pressure (> 50 bar) to produce fine water-mist jets. Discharge characteristics for this nozzle typology have been extensively studied, most notably by Lefebvre [8] and more recently by Yule and Widger [9]. Many parameters are of interest to perform a deep insight of these sprays. First and foremost, drop size represents a key point to quantify the atomization degree and to provide a useful input to a numerical code. Among the numerous works, Azzopardi [10] and Babinsky and Sojka [11] have discussed drop-size distribution from experimental, numerical and theoretical point of view. In this study, the conventional light-diffraction technique has been slightly modified to estimate the overall spray distribution: the *Malvern Spraytec* has been conveniently employed and drop-size measurements have been weighted over the volume-flux distribution, that has been measured by a mechanical patternator. This procedure has been aimed at reconstructing a flux-based characteristic diameter. Moreover, initial spray velocity has been investigated and determined by Particle Image Velocimetry (PIV). This technique has rarely been applied to the particular field of the present study; it is worth to mention Widmann et al. [12] and Sheppard [13], who have performed PIV tests on traditional-sprinkler sprays. However, initial velocity represents a very important parameter to quantify the spray momentum, that is a main discharge characteristic. Moreover, an evaluation of the spray-cone angle has been stressed out from PIV results. Both initial velocity and cone angle serve as input parameter in the employed compu-

[*] Corresponding author

tational codes. The experimental analysis has been deeply discussed in Santangelo et al. [14,15]. Numerical analyses of water-mist systems have been conducted over many applications [16-18], especially employing FDS (Fire Dynamics Simulator). However, the numerical approach has been mainly focused on predicting the flow-flame interaction, that practically means the suppression performance. Therefore, this work has been carried out to understand the code capability of properly simulating a water-mist spray. To this end, the already mentioned parameters have been set as the input and the measured volume-flux distribution has been employed as the validating tool.

Experimental apparatus and results

An experimental setup has been built to perform all the already mentioned measurements. The nozzle (Fig. 1a, no. 1) has been placed at 2 m height from the floor. This nozzle is constituted by 6 peripheral injectors and the central one: tests have been carried out on the spray produced by this latter. A tank (Fig. 1a, no. 2), an electric pump (Fig. 1a, no. 3) and a pressure gauge (Fig. 1a, no. 4) have been conveniently installed. A *Malvern Spraytec* particle sizer (Fig. 1a, no. 5) has been adjusted in order to have the laser beam at 1 m height from the floor. The PIV system consists of a laser emitter (pulsed 30 mJ Nd:YAG) and a thermo-electrically cooled CCD camera (14 bit, 4 Mpx). The laser emitter (Fig. 1a and 1b, no. 6) and the camera (Fig. 1b, no. 8) have been set to illuminate the initial region of the spray and to take images of the sampling area with no angular correction. Velocity maps have been reconstructed averaging a set of 300 double images. A data acquisition system has been provided (Fig. 1a and 1b, no. 7). Volume-flux distribution has been measured through a home made mechanical patternator, (Fig. 1b, no. 9). It is constituted by a set of 55 plastic tubes. The inlet section of every tube has been made perpendicular to the injector axis. The frame of the patternator has been adjusted to collect water at 1 m height from the floor: therefore, drop-size and volume-flux measurements are performed over the same spray cross section. The central tube has been placed right under the injector, so its axis was coincident with the injector one. The experimental campaign has been carried out to cover the already mentioned range of high operative pressure: tests have been run at 60, 70 and 80 bar. Operative pressure means the value reported by the pressure gauge, that practically represents the pressure right upstream the nozzle.

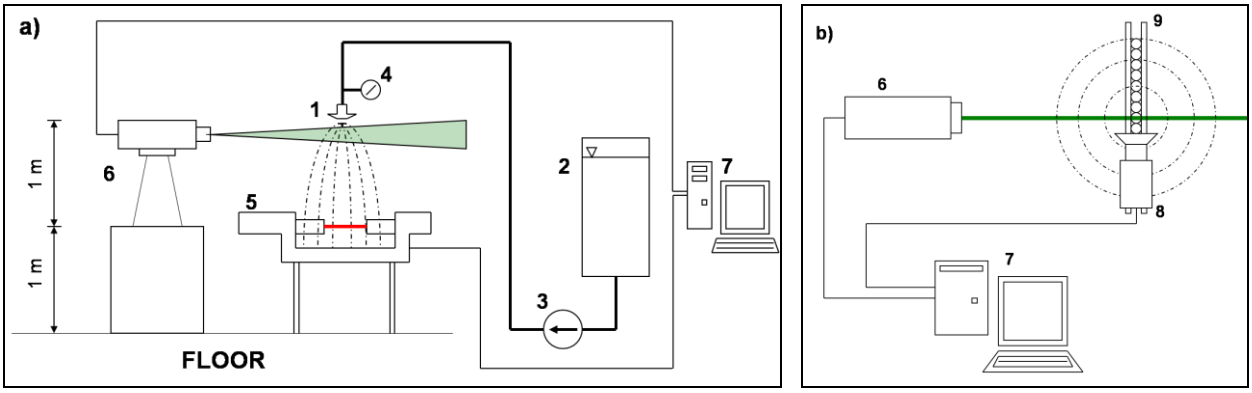

Figure 1. Sketch of the experimental facility: a) view from side (*Malvern Spraytec* and PIV system); b) view from above (PIV system and mechanical patternator).

An experimental methodology has been developed to gain a proper evaluation of the numerous parameters. A thorough description of any proposed procedure is presented in Santangelo et al. [15]. However, it is worthwhile to briefly summarize the main points. Drop-size measurements have been taken by the *Malvern Spraytec* at a prescribed number of radial locations, being this analysis based on hypothesis of symmetry for any spray cross section. The *Malvern Spraytec* has been placed to set its sampling volume perpendicular to the radial coordinate. Measurements have been carried on every 30 mm along a radius starting from the intersection between the injector axis and the spray cross section. The last location has been set at 120 mm from this intersection, because further there is only mist, that cannot be successfully detected by the *Malvern Spraytec*. Then volume-flux distribution has been measured by the mechanical patternator, that has been placed along a diameter of the spray cross section. The volume-flux results from the water collected in every tube during a prescribed amount of time. Hypothesis of diametrical symmetry has been applied. A center of volume flux has been calculated for each test: this point has been identified as the real center and it is not perfectly coincident with the intersection between the injector axis and the spray cross section, due to little experimental asymmetries. Finally, a curve of volume-flux distribution has been extrapolated to express this parameter as a function of the radial coordinate. Drop-size distribution has been reconstructed by

weighting drop-size measurements through volume-flux distribution. This procedure allows to obtain a proper evaluation of drop-size distribution as a result of an averaging process through another parameter (volume flux) and not only as a simple measurements by the *Malvern Spraytec*. A typical Rosin-Rammler log-normal distribution has been employed to predict the drop-size trend as a function of the volume fraction. This distribution is expressed as:

$$CVF = \begin{cases} (2\pi)^{-1/2} \int_0^{D_{CVF}} (\gamma' D)^{-1} e^{-\frac{[\ln(D/D_{v50})]^2}{2\gamma'^2}} dD & (D_{CVF} \le D_{v50}), \\ 1 - e^{-0.693(D_{CVF}/D_{v50})^{\gamma}} & (D_{v50} < D_{CVF}), \end{cases} \quad (1)$$

where D is the generic droplet diameter, CVF is the Cumulative Volume Fraction, γ is a curve-fitting coefficient and γ' is expressed as $\gamma' = 2((2\pi)^{1/2}(\ln 2)\gamma)^{-1}$. Suitable values for the curve-fitting γ coefficient have been determined to gain the best agreement between the experimental drop-size trend and the predictive function. As an example, Fig. 2 reports the reconstructed drop-size distribution at 80 bar of operative pressure.

The PIV experimental campaign has been carried out without any seeding, because water droplets produced by a pressure-swirl atomizer at high pressure are tiny enough to be tracking particles themselves. However, reliable values of velocity were practically obtained as of a distance of about 2 mm from the injector outlet along the axis. Fig. 3 shows the reconstructed PIV map at 80 bar.

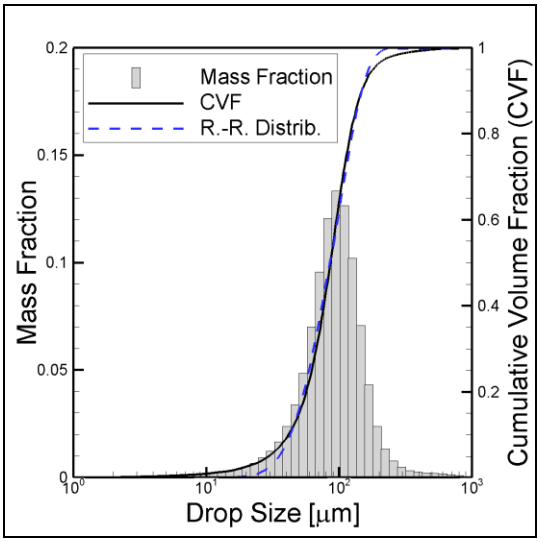

Figure 2. Drop-size distribution at 80 bar.

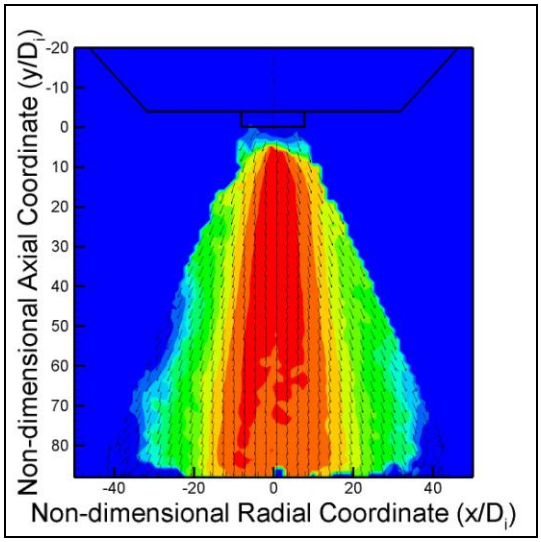

Figure 3. Reconstructed PIV map at 80 bar.

The velocity measurements have taken into account radial and axial components. Two-dimensional measurements of a three-dimensional vectorial parameter are based on the physical approximation that tangential component tends to become negligible once the flow leaves the injector. Angular velocity tends to decrease very fast once the generic particle (droplet) has been produced: thus, the tangential component can be neglected after a short axial distance from the injector outlet (around 5 mm). Velocity profiles have also been employed to determine the spray-cone angle and its trend along the axial extension of the PIV sampling area.

As a final summary, Table 1 reports the experimental values of the parameters of interest as inputs for the numerical simulations.

Table 1. Summary of the experimental input data for numerical simulations.

Operative Pressure [bar]	D_{v50} [μm]	γ Curve-fitting Coefficient	Initial Velocity [m s^{-1}]	Initial Spray-Cone Angle [°]
60	94.14	2.3	90.55	66.62
70	90.07	2.2	97.06	60.78
80	86.15	2.2	106.45	61.24

FDS Simulations: Description and Results

FDS is a CFD (Computational Fluid Dynamics) model of fire-driven fluid flow. This numerical tool has been developed by the National Institute of Standard and Technology (NIST) and is released a freeware program. It solves a form of the Navier-Stokes equations appropriate for low-speed thermally-driven flows applying a numerical procedure. Partial derivatives of mass, momentum and energy-conservation equations are approximated as finite differences, and the solution is updated in time on a three-dimensional, rectilinear grid. Turbulence can be modeled either through Large Eddy Simulation (LES) or Direct Numerical Simulation (DNS). In fact, performing DNS-based analysis requires an extremely fine numerical grid. Therefore, LES appears to be the most appealing approach to investigate large-scale applications. This technique is based on a direct model of transient large eddies, while eddies smaller than the grid scale are treated by a Smagorinsky form. In addition, FDS employs the Euler-Lagrangian method to model the particle transport. By this approach, trajectories of a representative number of droplets are predicted and momentum is transferred between the two phases (liquid and gaseous) applying the particle-source-in-cell method. FDS does not provide a physical simulation of droplet collision and break-up phenomenon. However, a semi-empirical model is introduced to simulate the droplet evaporation. Water droplets are inserted in a FDS model through a sprinkler (or a nozzle). Particle-size distribution is expressed as a function of Cumulative Volume Fraction (CVF): a Rosin-Rammler log-normal distribution (Eq. 1) is employed as a suitable mathematical representation. Finally, the flow number of the specific simulated nozzle serves as the parameter to compute the discharged mass-flow rate at the prescribed operative pressure. The flow number is strictly connected to the discharge coefficient, commonly used in the propulsion field as a way to express the effectively released mass-flow rate.

Some simulations employing FDS 5.2 were performed. A rectangular computational domain was set with dimensions of 1.0 m (x) by 1.0 m (y) and 2.0 m (z) height in a Cartesian coordinate. The injector has been set on the top of the z domain and centered on the x-y axes. The geometry was divided into 11 grids (Fig. 4), that becomes coarser moving from the injector. Starting from the injector: grid 1 is a cube consisting of 64000 cells (5 mm grid size); grid 2 is a cube consisting of 125000 cells (20 mm grid size); grids 3, 4, 5 and 6 are constituted by 20000 cells each with 20 mm grid size; grids 7, 8, 9 and 10 are constituted by 500 cells each with 40 mm grid size; finally, the grid 11, the closest to the floor, consists of 12,500 cells (40 mm grid size). All the boundaries of the geometry have been set as open vents except for the floor, that has been identified as a close surface. The droplets have been inserted 10 mm below the nozzle with the measured velocities. The input data to FDS was chosen from the scan of the entire spray. Furthermore, 30000 droplets per second have been released at intervals of 4.5 ms to model the water spray. The results of numeric simulations of the droplet mass flux at 1 meter from the nozzle are reported for three different operative pressures (60, 70 and 80 bar) and are compared with the related experimental data (Fig. 5). The diagram shows that the peak of droplet volume-flux distribution lies beneath the injector (z axis) for the values obtained with FDS prediction and close to this axis for the experimental values. This outcome is valid over the entire range of operative pressure. Moreover, the calculated values are about two times bigger than the measured ones. In terms of discrepancy between numerical and experimental results, FDS appears to overestimate the volume flux in a 40 mm radius from the centre (perpendicular to the injector) and then starts to underestimate the flux. The peak at70 bar is perfectly amid the ones at 60 bar and at 80 bar on experimental curves, while this trend is not exactly reproduced by FDS. As a matter of fact, the calculated values at 70 bar are closer to the ones computed at 80 bar in the numerical simulation.

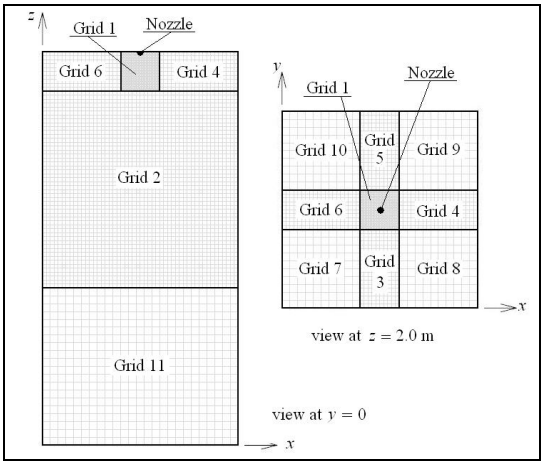

Figure 4. FDS computational grid.

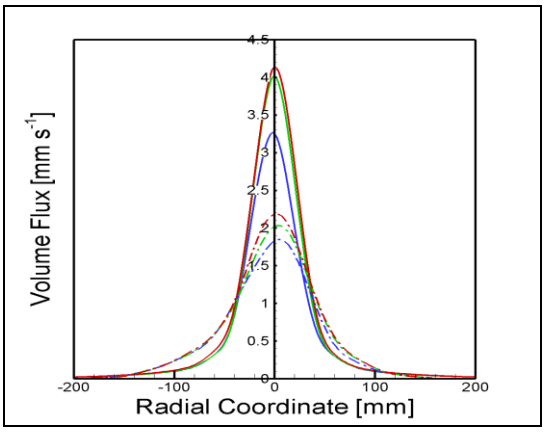

Figure 5. Comparison between experimental (dashed-dot) and FDS numerical (solid) volume-flux curves at 60 (blue), 70 (green) and 80 (red) bar.

Fluent® Simulations: Description and Results

The CFD commercial code Fluent® has been challenged in simulating a water-mist flow: very few works are available in the open literature about this task, even because this code is not usually applied in fire-protection field. The two-phase models implemented in Fluent® have been validated by comparing volume-flux distribution obtained numerically with experimental data, following the procedure previously described about FDS. Two different methods may be used to face a water-mist case: the Discrete Phase (DP) and the Eulerian Species Transport (EST) models. In the DP model, the particle phase is treated as the discrete phase within the Lagrangian scheme and the fluid phase as the carrier phase as in the Eulerian frame. Trajectories of individual particles can be calculated by the balancing forces acting on them. In the Lagrangian particle-tracking approach, particle-phase and fluid-phase interactions are accounted iteratively by updating the fields at predetermined intervals. The drying particle trajectories influenced by turbulence are predicted by the discrete random-walk tracking approach. A standard k-ε model has been employed to simulate turbulence within the fluid phase. The EST model in Fluent allows to model multiple separate interacting phases. Phases can be liquid, gas, or solid in almost any combination. A Eulerian approach is used for each phase, in contrast with the Eulerian-Lagrangian approach that is used for the DP model. The description of multiphase flow as interpenetrating continua incorporates the concept of phasic volume fractions. Volume fractions represent the space occupied by each phase and mass and momentum-conservation laws are obeyed by each phase individually. Derivation of conservation equations is performed by averaging the local instantaneous balance for each of the phases or by using the mixture-theory approach. The same k-ε model which simulates turbulence within the fluid phase in DP approach has been used to describe both phases in EST approach. In fact, only the EST model has been employed, as far as the available literature shows that it is the most appropriate for dense and tiny water droplets. Within the EST model approach, two different methodologies have been followed for geometry and boundary conditions. The geometry and the mesh have been generated using Gambit pre-processor, provided by Fluent® package. The domain was a cube 2.0 m by 2.0 m by 2.0 m. Wall boundary conditions have been set at top and floor surfaces of the domain, while symmetric boundary conditions have been set at the lateral surfaces of the computational domain. A water-mist outlet was installed at the centre of the top surface, with the shape of a small cylinder having the same diameter of the injector (3 mm) and 10 mm height. The mist droplets were injected from this cylinder with a 30° angle spreading. The water flow rate was 2 L/min. The geometry has been meshed using about 1000000 tetrahedral cells. With the second methodology, a volume with the same dimensions of the injector has been built and the production of droplets has been modeled as a mass-source term in correspondence to this volume. The source term has the same value of inlet mass-flow rate at the injector. The geometry of the rest of the domain is a cube 2.0 m by 2.0 m by 2.0 m. Wall boundary conditions have been set at top and floor surfaces of this domain, while symmetric boundary conditions have been set at the lateral surfaces of the computational domain The flow pattern within the spray cone is very complex, with high momentum transfer between water droplets and air and high turbulence.

The simulations are not able to get collision and coalescence of droplets, collapse of the spray and momentum transfer from droplets to air. Figure 6 shows the flow pattern of water droplets obtained following the first methodology. This approach leads to overestimate dimensions of the spray cone with respect to experimental results as well as droplet velocity distribution. The velocity profiles are bell-shaped, if plotted at a constant distance from the injector, as functions of the radial coordinate. The radius of the droplets velocity profile obtained by Fluent® is around 350 mm at a distance of 1 m from the injector outlet. A radius of 150 mm has been experimentally obtained. Velocity profiles by Fluent® under the first approach at a distance of 1 m from the injector outlet show a peak value of about 1 m s^{-1}, while the experiments show velocity peaks of about 2 mm s^{-1}. With the second methodology, a larger spray cone is obtained, while the droplet velocity distribution is in good agreement with the experiments. The radius of the spray cone at a distance of 1 m from the injector outlet is about 200 mm.

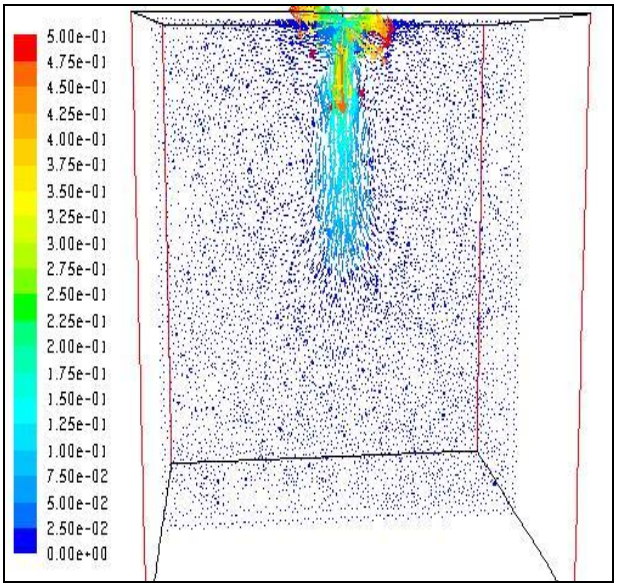

Figure 6. Velocity vectors of water droplets.

Fig. 7 shows a comparison between droplet volume flux obtained by Fluent® under the second approach at a distance of 1 m from the injector outlet. A good agreement between numerical and experimental data is stressed out, even if the computational code tends to generally overestimate this parameter. As far as this computational analysis by Fluent® represents a preliminary attempt, only the operative pressure of 80 bar has been considered in the numerical simulations.

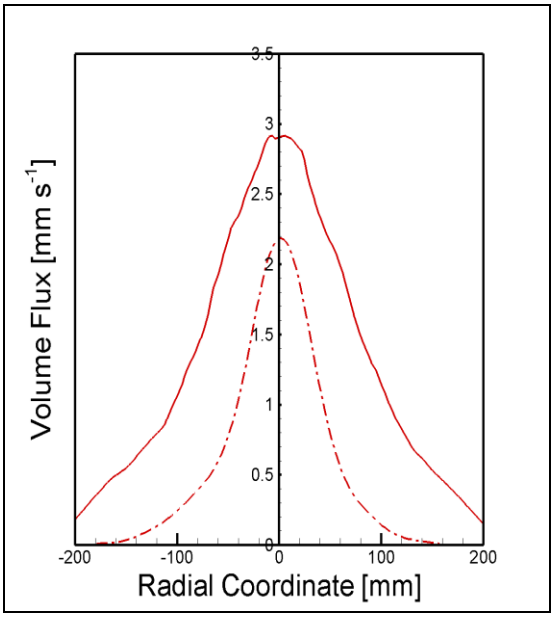

Figure 7. Comparison between experimental (dashed-dot) and Fluent® numerical (solid) volume-flux curves.

Concluding remarks

Experimental and numerical analyses have been conducted to investigate a water-mist spray. Experimental results have been obtained employing both laser-based diagnostics and *ad hoc* built instruments about drop size, volume-flux distribution, initial velocity and spray-cone angle. Computational simulations have been performed by FDS and Fluent® codes. Validation of numerical models has been carried out based on the volume-flux distribution: a good agreement has been obtained between FDS simulations and experimental results, while Fluent® shows promising results, but still-to-be-solved questions about modeling procedure. However, limits of the employed instrument have also to be taken into account: the mechanical patternator is incapable of collecting the most tiny droplets, so the experimental results tends to underestimate the total volume flux. Therefore, the overestimation provided by the numerical codes does not lead to a large discrepancy with the physical distribution.

Acknowledgments

The authors wish to thank Prof. André W. Marshall and Ning Ren (Dept. of Fire Protection Engineering, University of Maryland – College Park, USA) for their invaluable help throughout the experimental activity. Bettati Antincendio S.r.l. and Regione Emilia-Romagna (Italy) are also acknowledged for providing financial support to the present research.

References

1. Ndubizu, C.C., Ananth, R., Tatem, P.A., and Motevalli, V., *Fire Saf. J.* 31:253-276 (1998).
2. Adiga, K.C., Hatcher Jr., R.F., Sheinson, R.S., Williams, F.W., and Ayers, S., *Fire Saf. J.* 42:150-160 (2007).
3. Fisher, B.T. , Awtry, A.R., Sheinson, R.S., and Fleming, J.W., *Proc. Combust. Inst.* 31:2731-2739 (2007).
4. Lentati, A.M., and Chelliah, H.K., *Combust. Flame* 115:158-179 (1998).
5. Chelliah, H.K., *Proc. Combust. Inst.* 31:2711-2719 (2007).
6. Grant, G., Brenton, J., and Drysdale, D., *Prog. Energ. Combust. Sci.* 26:79-130 (2000).
7. Paulsen Husted, B., Ph.D. Thesis, Lund University, Lund, Sweden, 2007.
8. Lefebvre, A.H., *Atomization and Sprays*, Hemisphere, 1989.
9. Yule, A.J., and Widger, I.R., *Int. J. Mech. Sci.* 38:981-999 (1996).
10. Azzopardi, B.J., *Int. J. Heat Mass Transf.* 22:1245-1279 (1979).
11. Babinsky, E., and Sojka, P.E., *Prog. Energy Combust. Sci.* 28:303-329 (2002).
12. Widmann, J.F., Sheppard, D.T., and Lueptow, R.M., *Fire Technol.* 37:297-315 (2001).
13. Sheppard, D.T., Ph.D. Thesis, Northwestern University, Evanston, IL, USA, 2002.
14. Santangelo, P.E., Ren, N., Tartarini, P., and Marshall, A.W., *Twenty-fifth UIT National Heat Transfer Conference*, Trieste, Italy, June 2007, pp. 123-127.
15. Santangelo, P.E., Ren, N., Tartarini, P., and Marshall, A.W., *Twenty-second European Conference on Liquid Atomization and Spray Systems*, Como Lake, Italy, September 2008, paper 10-5.
16. Kim, S.C. and Ryou, H.S., *Build. Environ.* 38:1309-1316 (2003).
17. Hostikka, S., and McGrattan, K., *Fire Saf. J.* 41:76-86 (2006).
18. Shi, C.L., Lu, W.Z., Chow, W.K., and Huo, R., *Int. J. Heat Mass Transf.* 50:513-529 (2007).